# PathoSPOT genomic surveillance reveals under the radar outbreaks of methicillin resistant *S. aureus* bloodstream infections

Ana Berbel Caban, MD [1*], Theodore Pak, MD, PhD [2*], Ajay Obla, PhD [2], Amy Dupper, MA MPH [1], Kieran I. Chacko, PhD [2], Lindsey Fox, MD [1], Alexandra Mills, MD [1], Brianne Ciferri, MPH[2], Irina Oussenko, PhD [2], Colleen Beckford, MS [2], Marilyn Chung, MS [2], Robert Sebra, PhD [2,3,4,5], Melissa Smith, PhD [2,3], Sarah Conolly [6], Gopi Patel, MD [1,6], Andrew Kasarskis, PhD [2,3,7], Mitchell J. Sullivan, PhD [2], Deena R. Altman, MD, MS [#1, 2], Harm van Bakel, PhD [#2,3]

1. Department of Medicine, Division of Infectious Diseases, Icahn School of Medicine at Mount Sinai, New York City, NY, USA
2. Department of Genetics and Genomic Sciences, Icahn School of Medicine at Mount Sinai, New York City, NY, USA
3. Icahn Institute for Data Science and Genomic Technology, Icahn School of Medicine at Mount Sinai, New York, NY 10029, USA
4. Black Family Stem Cell Institute, Icahn School of Medicine at Mount Sinai, New York, NY, 10029, USA
5. Sema4, a Mount Sinai venture, Stamford CT, 06902
6. Infection Prevention, The Mount Sinai Hospital, New York City, NY USA
7. Department of Population Health Science and Policy, Icahn School of Medicine at Mount Sinai, New York City, NY, USA

* These authors contributed equally to this work

\# These authors are co-senior authors on this work

**Correspondence**:

Harm van Bakel (harm.vanbakel@mssm.edu)

**Keywords**

whole genome sequencing, visualization toolkits, MRSA bacteremia

# Abstract

Whole genome sequencing (WGS) is increasingly used to map the spread and transmission dynamics of human pathogens, especially in nosocomial settings. A limiting factor for more widespread adoption of WGS for infection prevention practices is the availability of standardized tools for genome analysis. Here we present PathoSPOT, which integrates genomic and electronic medical record (EMR) data for rapid detection of nosocomial outbreaks and analysis of epidemiological timelines. To demonstrate its capabilities we analyzed complete genomes obtained from long-read sequencing of 197 invasive MRSA (bacteremia) cases from two hospitals during a two-year period. PathoSPOT identified 8 clonal clusters that had not been identified by epidemiological data, encompassing 33 patients (16.8%). The largest cluster was consistent with an outbreak of a hospital-associated ST105 MRSA clone among 16 adult patients in multiple wards. Timeline and location data suggested that an early outbreak event led to infection and long-term colonization of multiple cases, followed by transmissions to other patients during subsequent hospitalizations. Overall, we find that PathoSPOT can detect outbreaks that are not readily apparent from epidemiological data and contribute to morbidity and mortality. When applied as part of comprehensive ‘real-time’ sequencing-based surveillance, PathoSPOT may play an important role in understanding the complexities of pathogen transmission dynamics and enable timely interventions.

# Introduction

The utility of whole genome sequencing to track transmissions and outbreak events is well-established, in particular for highly clonal pathogens such as *S. aureus,* where classical molecular typing methods such as multi-locus sequence typing (MLST) and pulsed-field gel electrophoresis (PFGE) do not provide enough resolving power (Eyre et al. 2012; Harris et al. 2010; Köser et al. 2012; Sullivan et al. 2019). Despite the increased use of WGS, bottlenecks remain that complicate its use in managing nosocomial outbreaks. Comparative genome analyses often require specialized knowledge and/or selection of appropriate reference sequences. Analysis and visualization frameworks are available to aid genome analysis in outbreak settings (Hadfield et al. 2018; Zhou et al. 2018; Lees et al. 2019), but these are less suited for nosocomial settings where genomic results need to be integrated with detailed epidemiological results and patient histories to trace movements and contacts. This can be time-consuming, especially when relying on manual chart review. Integration with electronic medical record (EMR) systems can facilitate this process, but tools that combine epidemiological and genomic information in a comprehensive manner for nosocomial outbreak tracking are not readily available.

To facilitate detection and visualization of transmissions in nosocomial settings we developed an open-source toolkit called PathoSPOT (Pathogen Sequencing Phylogenomic Outbreak Toolkit), which combines automated comparisons of complete or draft genomes with interactive visualization of clonal clusters. Further integration of epidemiological data enables high resolution analysis of outbreak phylogenies and timelines. Since methicillin resistant *Staphylococcus aureus* (MRSA) is a common cause of healthcare-associated (HA) infections in the USA that pose a potentially fatal threat to patients, we used our toolkit as part of a complete genome screening program of MRSA blood isolates, based on long-read sequencing. During a 24-month period, we obtained finished-quality MRSA genomes from 197 bacteremic patients at two urban hospitals in New York City. PathoSPOT analysis identified 8 clusters of highly related isolates that had not been recognized before based on available epidemiological information; the most extensive cluster encompassing 16 patients. In-depth analysis with PathoSPOT allowed us to reconstruct the outbreak timeline and identify common links among these individuals. Our findings demonstrate the utility of PathoSPOT for infection prevention efforts in health systems and highlight the role of colonization in long-term nosocomial outbreaks.

# Results

## MRSA surveillance with PathoSPOT identifies frequent under the radar transmissions

We developed PathoSPOT to enable automatic comparisons of large numbers of complete or draft microbial genomes, and to rapidly identify closely related isolates indicative of transmission events and map their epidemiological timelines (**Fig. 1A**). PathoSPOT combines existing tools for whole genome comparison and alignment with custom analysis and visualization code developed in Ruby, Python, and Javascript (https://pathospot.org). To demonstrate its utility, we applied PathoSPOT to whole-genome surveillance data obtained from all MRSA isolates from bacteremic cases at two hospitals (A and B) during a 2-year period. In total we sequenced 224 genomes for 221 isolates from 197 patients using PacBio long-read technology and obtained 184 finished-quality and 40 draft genome sequences (**Table S1**). In most cases we only sequenced the primary blood culture, but additional isolates were sequenced for the same patient in cases of prolonged or recurrent infections. We first used the PathoSPOT “compare” pipeline to cluster genomes based on their Mash distance (Ondov et al. 2016). This step groups highly related genomes prior to multi-genome alignment and avoids the need for manual selection of a reference genome. The Mash distance threshold for MRSA was determined empirically to yield clusters of genomes consistent with clonal complex assignments based on MLST data, and to maximize core genome alignments in each cluster (**Fig. 1B**). Pairwise distances between genomes were then calculated as the number of single nucleotide variants (SNVs) between core genome alignments in each cluster for further analysis.

To identify transmission events we used the PathoSPOT “heatmap” tool (**Fig. 2**). We set a threshold of ≤15 SNVs to identify potential transmissions, based on the extent of intra- and inter-patient variability we previously observed in complete genome analysis of an extended outbreak (Sullivan et al. 2019), and considering a core genome mutation rate of ~3 SNVs per Mb per year (Harris et al. 2010; Young et al. 2012). The distance threshold can be varied interactively in the heatmap tool to explore grouping at different levels of relatedness, depending on the pathogen. At the selected threshold we identified 8 clonal clusters with a total of 33 patients, amounting to an overall transmission rate of 16.8% (**Fig. 2C**). Most clusters consisted of patient pairs (5/8) but there were 3 with more than two patients. Patients within each cluster typically had overlapping visits (75%) and stayed in the same wards at some point during these visits (63%), but in many cases MRSA bacteremia was only found after they had transferred to

different wards. This likely contributed to the fact that none of the clusters had been recognized epidemiologically. The most striking example of this was a clonal cluster of 16 patients, based on data from 24 isolates obtained from 9 wards over a period of 21 months.

## PathoSPOT timeline highlights the role of colonization in prolonged MRSA outbreaks

The presence of a clonal MRSA cluster among 16 bacteremia cases was consistent with a prolonged "under the radar" outbreak. The outbreak strain was a clone of the hospital-associated USA100 lineage (*spa* type t002, MLST 105, staphylococcal cassette chromosome *mec* type II) and resistant to fluoroquinolones, oxacillin, clindamycin, erythromycin and gentamicin based on automatic microbroth dilution testing. We next used the PathoSPOT "dendro-timeline" tool, which combines phylogenetic analysis of outbreak isolates with the full admission/transfer/discharge (ADT) history for each patient, to analyze this outbreak in more detail (**Fig. 3**). The PathoSPOT core genome dendrogram, derived from the multigenome alignment of the superset of isolates in the same Mash cluster, indicated the presence of distinct subclades within the outbreak (**Fig. 3A**). Shared variant profiles within each subclade were consistent with sub-transmissions within the larger outbreak (**Fig. 3A**). Isolates from p176, who tested positive for MRSA bacteremia numerous times within a span of 6 months, were represented in distinct clades, suggesting that this patient carried multiple variants of the outbreak strain at the same time. This was confirmed by sequencing two subclones from p176 isolate ER05682 (Fig. 3A, ▲ and ♦).

Based on the PathoSPOT timeline of events (**Fig. 3B**), we reconstructed the most likely outbreak scenario (**Fig. 3C**). The first two cases (p40 and p574) tested positive on ward 8. No other positives were found on this ward, but five other cases had overlapping stays (p176, p459, and p181) or were admitted to the same ward within four weeks of the first positive test (p34, p142). All but one patient tested positive for bacteremia within seven weeks of their stay in ward 8, following transfers or readmissions to other wards. Strikingly, p459, who was discharged from ward 8 four days after the initial positive case, did not present with bacteremia until 20 months later. In the intervening period this patient had no contact with our health system except for two dermatology office visits where positive wound cultures for MRSA were obtained. The degree of genetic drift of the p459 isolate (11 SNVs) and pattern of positive wound cultures prior to bacteremia are consistent with long-term colonization after initial exposure in ward 8, although we could not verify this scenario as the wound isolates were not available for sequencing.

Five additional patients tested positive in wards 16, 2, and 12 during the first six months of the outbreak (**Fig. 3B, 3C**). Each instance was preceded by the transfer of an outbreak case that had previously stayed in ward 8, suggesting that direct or indirect transmissions from these cases propagated the outbreak. Patient p34 was transferred from ward 8 to ward 16, into a room neighboring p628, who became bacteremic two days later. Both their isolates were grouped in the same subclade (**Fig. 3A**, ▼). Likewise, p142 was transferred from ward 8 to ward 2, where there was overlap with p399 and p476 before all three became bacteremic on this ward. Notably, p142 and p176 overlapped with p476 on two different days in the inpatient hemodialysis unit, providing an alternative acquisition route. Finally, after discharge from ward 8, p181 was readmitted to ward 12, where the patient overlapped stays with patients p2 and p669.

From months 7 to 21, four additional transmissions were identified. Patient p176 tested positive for the outbreak strain on multiple occasions during readmissions and was implicated in two other potential transmissions. The patient visited the emergency department (ED) on the same day as patient p648, and had an overlapping stay in ward 2 with p593 for at least 5 days, in the months prior to their positive tests. Following readmission after a 20-month hiatus, p459 likely transmitted to p10, based on evidence of an overlapping stay in ward 36 (**Fig. 3B**) and the high relatedness of their isolates (**Fig 3A**, **+**). Patient p77 is the only person that did not have overlapping stays with other outbreak cases. The patient had a total of two pediatric (ward 49) and one adult (ward 2) admission to the hospital within 21-months. Given that all other outbreak cases were adults, we consider ward 2 the most likely location of MRSA acquisition, where p77 shared healthcare workers with p593 who was admitted to the same unit 11 weeks before.

Altogether, PathoSPOT analysis suggested that initial exposure in Ward 8 resulted in colonization and clinical infection of up to 7 cases (44% of the prolonged outbreak cluster), followed by secondary transmissions after ward transfers and/or subsequent hospital visits of these initial cases. The alternative scenario of community transmissions was assessed by mapping of home zip codes, which indicated that 13 of 16 cases lived in different areas, including 5 that lived outside of New York City. Spatiotemporal analyses of the seven smaller clusters (**Fig. S1**) showed that five include direct overlaps in wards or outpatient settings, of which three are plausible transmission events, and two such events are months before the clonal blood cultures were obtained. Taken together, our data suggest that in the absence of genomic surveillance, MRSA transmission within a healthcare setting often goes undetected as asymptomatic colonization, only leading to clinically apparent infections weeks to months later.

## Hand hygiene compliance and vascular access implicated in under-the-radar outbreak

As the prolonged outbreak extended over multiple wards, we further investigated hand hygiene rates, shared HCW, patient movements, and clinical characteristics. Average hand hygiene compliance in the wards associated with the majority of cases ranged between 79-83%. Compliance in wards 8 and 16 was reduced to 70% and 66% in the month prior to the first outbreak case, while ward 2 compliance was maintained at 79%. All outbreak patients shared at least one HCW involved in the care of other patients in the cluster. This is consistent with the high degree of overlapping stays in the same ward and suggests that direct and indirect transmissions may have played a role in propagating the outbreak. Although outbreak cases were moved frequently between units based on transfer records, they did not move more frequently than non-outbreak patients.

Chart review of outbreak cases revealed that 69% (n=11) were male, 75% (n=12) had been admitted from home, and 63% (n=10) had a hospital admission in the 90 days prior (**Table 1**). 75% (n=12) were considered hospital-onset (HO)-MRSA as defined by NHSN (Center for Disease Control and Prevention 2018) and 88% (n=14) of subjects had an invasive device at the time of infection. Notable was the presence of active malignancy (57%; n=8) including five persons with leukemia (4 acute myeloid leukemia, 1 chronic lymphocytic leukemia), and others with multiple myeloma (n=1), disseminated Kaposi sarcoma (n=1), and metastatic breast cancer (n=1). Among patients with hematologic malignancies, three had undergone hematopoietic stem cell transplant. The most common presumed source of bacteremia was vascular access (n=9; 56%), followed by skin source (n=4; 25%). The 90-day mortality incidence was 25% (n=4), of which 75% (n=3) was related to bacteremia with outbreak strain. We performed univariate and multivariate analyses of the 16 outbreak cases compared with 34 unique patients infected with non-outbreak ST105 MRSA during the same time period. Outbreak patients were significantly associated with HO-MRSA (OR= 5.20 95% CI [1.04-26.01]; p=0.04) and the administration of intravenous chemotherapy prior to bacteremia (OR=11.24 95% CI [1.72-73.28]; p=0.01) in multivariate analysis. There were no differences in outcomes between outbreak and non-outbreak patients.

# Discussion

We developed the PathoSPOT phylogenomics toolkit to facilitate detection of outbreaks and transmissions as part of an ongoing genomics-based pathogen surveillance program. Application of the toolkit to 197 patients with MRSA bacteremia over a two-year period shows that under-the-radar transmission events are important sources of morbidity and mortality. Since precise construction of epidemiological timelines is labor intensive and time consuming, when implemented, our toolkit can avoid these bottlenecks and assist infection prevention staff with rapid identification of transmission events.

During the study period, PathoSPOT detected 8 clusters of MRSA involving 33 patients with bacteremia. A large outbreak impacted 16 patients from distinct adult medicine wards and spanned nearly the entire study period. In the absence of routine patient, HCW and environmental screening it was not possible to determine the original source of transmission cascade. Ward overlap was a key factor in forward transmissions, with a delay between exposure and subsequent bacteremia that sometimes extended for several months and likely played a role in obscuring the outbreak from epidemiological detection. Most wards involved had lower hand hygiene rates surrounding key outbreak events. Additional contributing factors likely included frequent patient movements and shared HCW. Frequent room changes within and between wards may also have resulted in contaminated environmental surfaces, which has been shown to play a role in the transmission of hospital pathogens (Otter et al. 2011, 2013).

Our study suggests a role for colonization in the progression and persistence of long term outbreaks (Senn et al. 2016; Merrer et al. 2000). Skin colonization may have played a role in acquisition, as the majority of presumed patient sources of bacteremia were central venous access or skin source. The number of patients with malignancies was also notable, particularly hematological with bone marrow suppression. Patients with hematologic malignancies have an increased risk of bacteremia, as central venous catheters remain an essential tool for their treatment, frequently leading to catheter-related infections (Zakhour et al. 2016).

The detection of nosocomial transmissions and outbreaks is critical for healthcare organizations. Precise, genomics-based, pathogen surveillance programs supported by rapid analysis frameworks such as provided by PathoSPOT are essential to detect events that are not readily ascertained by conventional infection prevention methods. Such programs would be more

effective when implemented across regional health systems, long-term acute care hospitals, and skilled nursing facilities, to track dissemination of strains and identify sources and at-risk patients based on contact networks. When combined with timely intervention, these efforts could help reduce endemic rates of nosocomial infections.

# Methods

## Ethics statement

This study was reviewed and approved by the Institutional Review Board of the Icahn School of Medicine at Mount Sinai.

## Bacterial culturing, DNA extraction and sequencing

Isolates were cultured and identified as part of standard clinical testing procedures in the Mount Sinai Hospital Clinical Microbiology Laboratory (CML), and stored in tryptic soy broth (TSB) with 15% glycerol at -80°C. Selected isolates were subcultured on tryptic soy agar (TSA) plates with 5% sheep blood (blood agar) (ThermoFisher Scientific) under nonselective conditions. The Qiagen DNeasy Blood & Tissue Kit (Qiagen) was used for DNA extraction, as previously described (Sullivan et al. 2019). Following quality control, DNA and library preparation, long-read sequencing was performed on the Pacific Biosciences RS-II platform to a depth of >200x.

## Genome assembly

PacBio SMRT sequencing data were assembled using a custom genome assembly and finishing pipeline (https://github.com/powerpak/pathogendb-pipeline), as previously described (Sullivan et al. 2019).

## Comparative genome analysis using PathSPOT-compare

We developed the PathoSPOT-compare pipeline to perform comparative phylogenomic analysis of finished, annotated genome assemblies for the specific purpose of outbreak detection. The pipeline is implemented as a Rakefile (a Makefile for the Ruby language) that calculates

dependencies and executes all necessary subtasks to reach desired outputs. PathoSPOT-compare takes FASTA-formatted genome assemblies as input, along with a relational database (SQLite or MySQL) containing metadata for each assembly (including collection time, location, collection method, organism, and patient ID), as well as metadata on patient ADT history (for spatiotemporal analysis).

Genetic distances for outbreak detection are ultimately calculated by counting SNP differences within core genome alignments; however, there is a trade-off between aligning increasingly diverse assemblies and a diminishing core genome size (as more subsequences will fail to align across all assemblies). Therefore, we implemented a hybrid approach, wherein pairwise distances between all assemblies are first estimated using Mash (Ondov et al. 2016), which uses a k-mer based hashing approach that approximates average nucleotide identity (ANI). Mash distances are used to perform greedy single-linkage hierarchical clustering, with clusters capped at a pre-specified diameter and size. The default parameters, which are also the parameters used for this study, are a maximum Mash cluster diameter of 0.02 (approximating 98% ANI among all included genomes) and at most 100 genomes per cluster.

Rapid core genome alignments are then created for each cluster using parsnp (Treangen et al. 2014), which is tailored for intraspecific genome analysis and is therefore well-suited for outbreak analysis. Outputted variant call files (VCF) for each cluster are converted to NumPy arrays (NPZ files) for fast loading and subsetting of variant data by PathoSPOT-visualize, the downstream visualization web application that can display called variants alongside phylogenies. The primary output for PathoSPOT-visualize is a JSON file containing a matrix of pairwise SNP distances for all genomes (with inter-cluster distances left unspecified) and a maximum-likelihood phylogeny for each cluster. Additional optional pipeline tasks export patient location data (as TSV files) and epidemiologic data on positive and negative culture results (as JSON files), both of which are automatically utilized and layered onto the comparative genomic analyses within PathoSPOT-visualize when available.

### Interactive detection and visualization of outbreaks with PathoSPOT-visualize

To visualize the above analyses as depicted in **Fig. 2, 3A-B, S1, and S2**, we created the PathoSPOT-visualize interactive web application. The application uses PHP scripts and AJAX to serve data from the JSON, TSV, and NPZ output files generated by the PathoSPOT-compare pipeline, which are then dynamically mapped to interactive HTML5 and scalable vector graphics

(SVG) elements using the D3.js (Data-Driven Documents) framework. All views are rendered in the browser, allowing the user to alter settings that trigger live animated transitions, and an intuitive sense of how changes propagate between the linked views of data.

There are three main user interfaces, the “heatmap” tool, the “network map” tool and the “dendro-timeline” tool. Users initially interact with the “heatmap” tool, which starts with selection of a dataset that can be prefiltered by specimen location, MLST, and time interval. The user can dynamically adjust the SNP threshold that specifies the genetic distance deemed suspicious for transmission; this process is aided by a histogram depicting distributions of SNP distances among same-patient isolates (generally expected to be related) and different-patient isolates (which are not, assuming a low level of transmission). This threshold is used to perform single-linkage hierarchical clustering of genomes on the client-side, with the clusters assigned random colors and depicted on a beeswarm timeline plot and a large heatmap of pairwise distances among all selected genomes. This large heatmap can be swapped for the “network map” view (**Fig. S2**), which plots genomes by their collection location in a geospatial layout, overlaid with density plots of overall epidemiological incidence and force-directed network links depicting genetic relationships.

Epidemiological links within the clusters can be further explored in the “dendro-timeline” tool, which combines a traditional phylogenetic dendrogram with a SNP matrix, a mapping of SNP locations onto a reference assembly, and a pannable-zoomable timeline of patient locations over time, with spatiotemporal overlaps highlighted as bright arcs. The phylogeny for the “dendro-timeline” tool is extracted from the larger maximum-likelihood trees built by parsnp, based on the SNP threshold and clustering parameters that the user selected in the “heatmap” tool.

## Case review

We performed a retrospective clinical chart review on all adults (age $\geq$18) subjects identified with MRSA bacteremia. Analyses were performed in SAS (v9.4)(SAS Institute 2013). Variables were analyzed initially in a univariate logistic regression model. Variables $p \leq 0.2$ were then placed into a stepwise multivariate logistic regression model (Dupper et al. 2019). An additional in-depth chart review was performed for subjects identified as being involved in transmission events. These details included location (ward, room, bed), all ADT information, procedures, and providers. Whole genome sequencing was performed on 1st patient blood isolate positive for

MRSA as part of an ongoing genomic surveillance program as described in (Sullivan et al. 2019). Hand hygiene is monitored by the Infection Prevention and Control department by the use of anonymous observers using the Joint Commision's Targeted Solutions Tool (TST) (Anderson et al. 2019), which was implemented in November 2014. This tool allows the staff member to document reasons for non-compliance and target areas of interventions. Hand hygiene observations are collected anonymously at entry and exit by trained staff members in each hospital ward. Hand hygiene rates were compared using a one-sample t-test.

### Data availability

All study data is available at https://www.pathospot.org.

### Software

The PathoSPOT-compare and PathoSPOT-visualize packages developed for this study are both open source and can be obtained from:

- https://github.com/powerpak/pathospot-compare
- https://github.com/powerpak/pathospot-visualize

A live demo of all visualizations created for this study, along with documentation on setting up and using the software with example data from this study, can be found at https://pathospot.org.

## Acknowledgements

This research was supported in part by R01 AI119145 (H.v.B.), the Icahn Institute for Genomics and Data Science (A.K.), the CTSA/NCATS KL2 Program (KL2TR001435, Icahn School of Medicine at Mount Sinai; D.R.A), and the New York State Department of Health Empire Clinical Research Investigator Program (Awarded to Judith A. Aberg, Icahn School of Medicine at Mount Sinai; D.R.A.) and F30 AI122673 (T.R.P.). The Research reported in this paper was supported by the Office of Research Infrastructure of the National Institutes of Health (NIH) under award numbers S10OD018522 and S10OD026880 as well as institutional funds. The funders had no role in study design, data collection and interpretation, or the decision to submit the work for publication.

# Figures

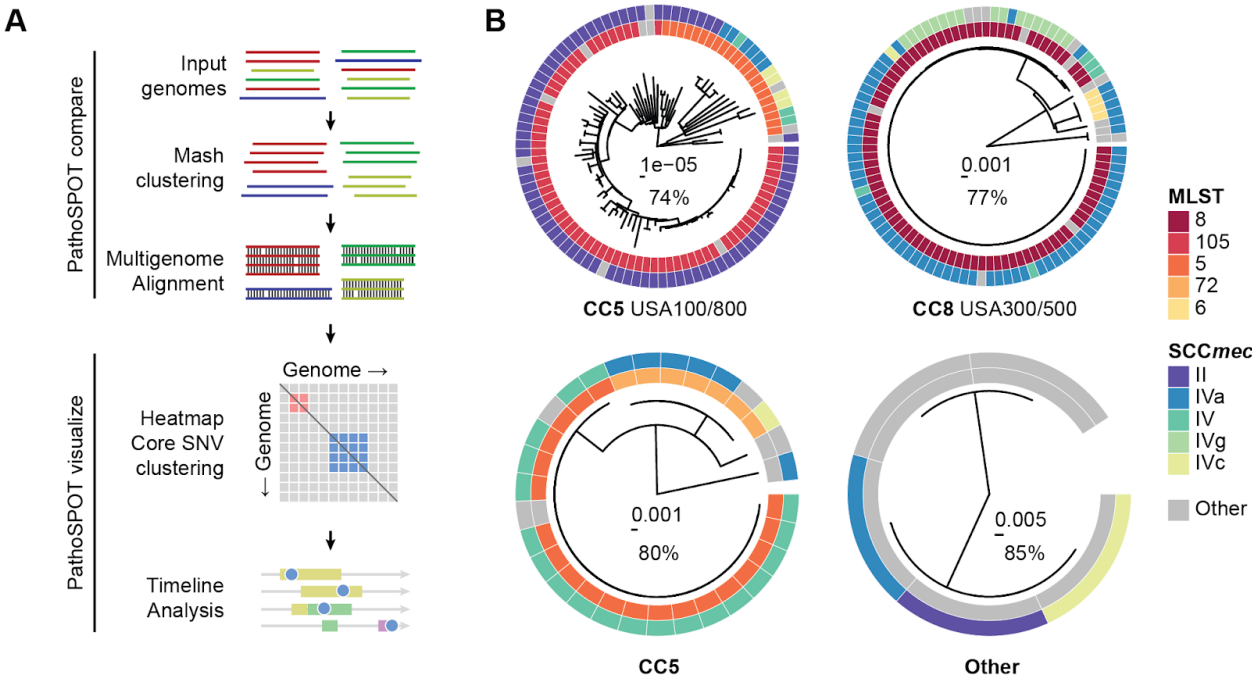


Figure 1. PathoSPOT comparative genome analysis of 221 MRSA isolates

**A)** Overview of the PathoSPOT whole-genome comparison framework. **B)** Maximum-likelihood phylogenetic trees produced from core genome SNVs identified from Parsnp whole-genome alignments of 4 clusters identified at a Mash score threshold of 0.02. Trees are annotated with MLST and SCC*mec* information (key shown on right) and clonal complexes (bottom). Scale bars indicating the number of substitutions per site in the phylogeny and the percentage of core genome coverage among all sequences is shown at the center of each tree.

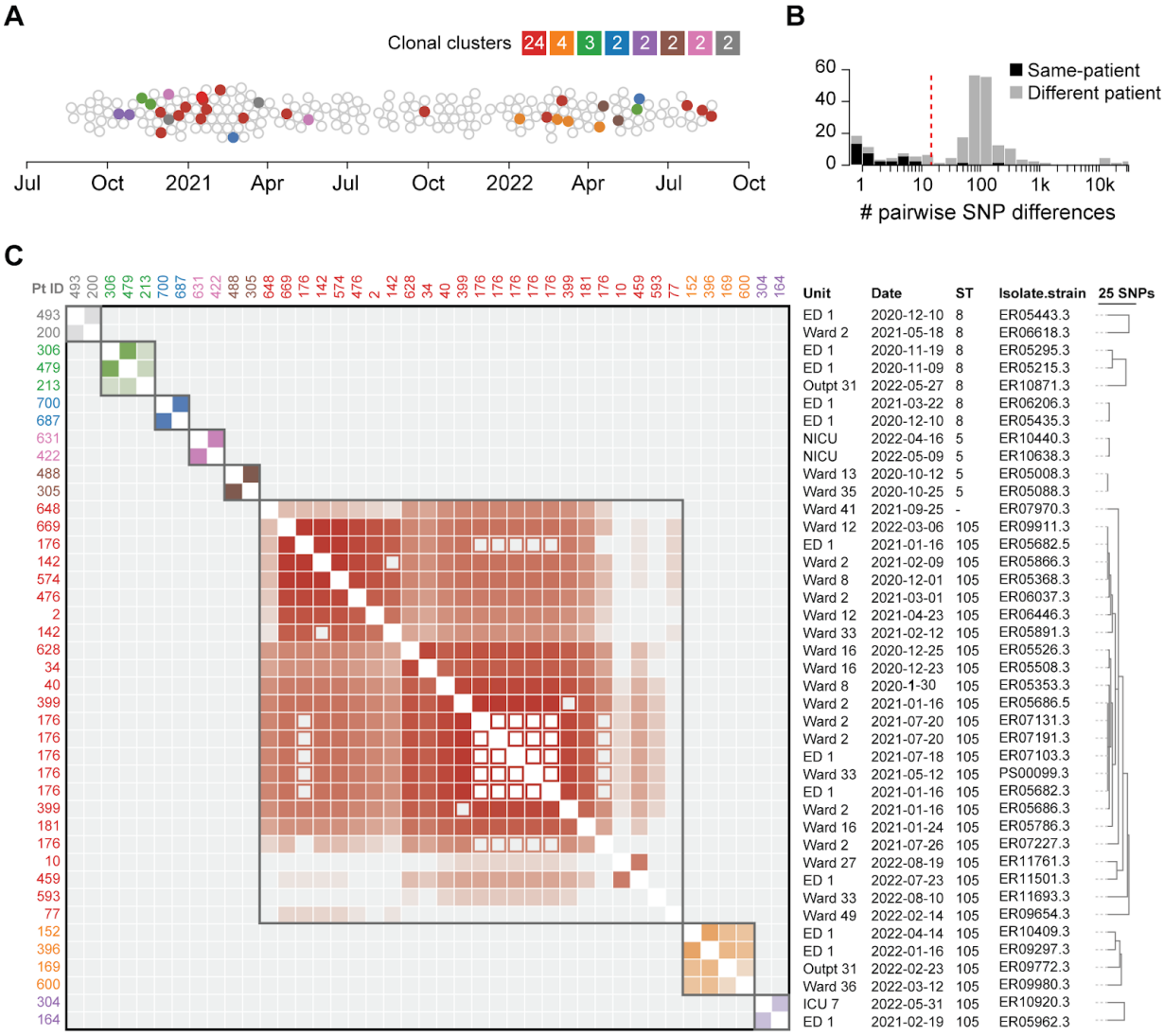


348 Figure 2. Identification of clonal clusters among 197 MRSA bacteremia cases

349 **A)** Beeswarm plot of MRSA cases with sequenced isolate genomes during the surveillance
350 period. Cases with isolates separated by ≤15 core genome SNPs are grouped in clonal clusters,
351 each highlighted with a distinct color. The number of isolates in each cluster is indicated in the
352 color key. **B)** Histogram of pairwise core genome SNP distances for isolates obtained from the
353 same patient (black bars) and isolates obtained from different patients (grey bars). The vertical
354 red line indicates the 15-SNP threshold for clonality. **C)** Heatmap of pairwise core genome SNP
355 distances between clustered isolates. Clusters are grouped along the diagonal and colored as in
356 A, with decreasing shading reflecting an increased pairwise SNP distance. Closed squares and

357 open squares are used for isolates from different patients or the same patient, respectively. All
358 date information in this figure was recoded to protect health information.

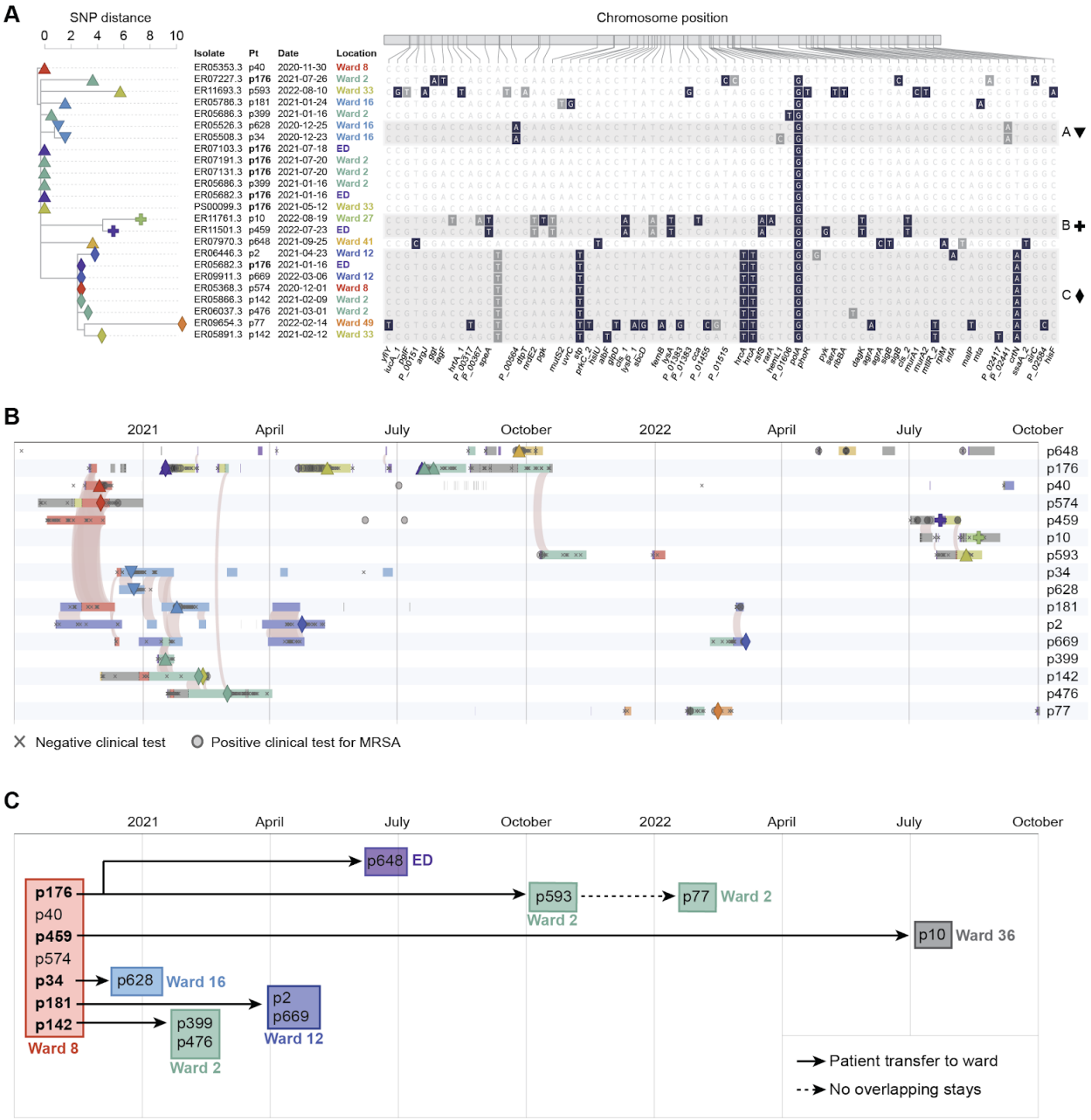


359 Figure 3. Epidemiologic timeline of long-term outbreak.

360 **A)** Phylogenetic tree of core genome SNP differences (left) with corresponding locations of each
361 variant relative to the first outbreak isolate that was obtained from p40 (right). Non-synonymous
362 and synonymous variants are highlighted in black and grey, respectively. Distinct clades with
363 three or more shared variants are shown as shaded areas (key on right). **B)** Epidemiologic
364 timeline reconstructed by PathoSPOT integration of genomic and epidemiological data. Rows

correspond to patients, with admission periods in hospital wards shown as horizontal bars. Wards are colored as in A. Sequenced clinical isolates are shown as different symbols matching those used in the phylogenetic tree in A, and colored according to the collection ward. Shaded arcs signify ward-level patient overlap within 24 hours. Other positive or negative clinical test results are indicated by grey symbols, with a key shown below. The timeline scale is shown at the top. **C)** Summary of key outbreak events in wards, derived from the epidemiological timeline. See main text for details. All date information in this figure was recoded to protect health information.

373 Table 1. Outbreak patients vs. patients with MLST 105 between January 2016 through
374 December 2017

| Factor | Outbreak Patients N = 16 (%) | Non-Outbreak Patients N = 34 (%) | Univariate Analysis OR (95% CI) | p value | Multivariate Analysis OR (95% CI) | p value |
|---|---|---|---|---|---|---|
| Male | 11 (69) | 21 (62) | 1.36 (0.39-4.82) | 0.63 | | |
| *Race/Ethnicity* | | | | | | |
| Non-Hispanic White | 5 (31) | 14 (41) | Reference | | | |
| Non-Hispanic Black | 3 (19) | 9 (26) | 0.93 (0.18-4.90) | 0.94 | | |
| Hispanic/Latino/Asian | 5 (31) | 6 (18) | 2.33 (0.49-11.17) | 0.29 | | |
| Unknown | 3 (19) | 5 (15) | 1.68 (0.29-9.75) | 0.56 | | |
| *Age at Time of Infection* | | | | | | |
| 18-54 Years | 6 (38) | 7 (21) | Reference | | | |
| 55-69 Years | 5 (31) | 9 (26) | 0.65 (0.14-3.04) | 0.58 | | |
| ≥ 70 Years | 5 (31) | 18 (53) | 0.32 (0.07-1.41) | 0.13 | | |
| History of IV Drug Use | 2 (13) | 2 (6) | 2.29 (0.29-17.90) | 0.43 | | |
| HIV | 1 (6) | 3 (9) | 0.69 (0.07-7.19) | 0.76 | | |
| *Admission Source* | | | | | | |
| Home | 12 (75) | 17 (50) | Reference | | | |
| NH/Rehab/LTACH | 2 (13) | 11 (32) | 0.26 (0.05-1.38) | 0.11 | | |
| Other Hospital | 2 (13) | 6 (18) | 0.47 (0.08-2.75) | 0.40 | | |
| Prior Hospital Admission (90 Days) | 10 (63) | 23 (68) | 0.80 (0.23-2.76) | 0.72 | | |
| *NHSN Definitions* | | | | | | |
| CO-MRSA | 4 (25) | 24 (71) | Reference | | Reference | |
| HO-MRSA | 12 (75) | 10 (29) | **7.20 (1.87-27.79)** | **0.004** | **5.20 (1.04-26.01)** | **0.04** |
| [A] Presence of Invasive Device | 14 (88) | 27 (90) | 0.78 (0.12-5.21) | 0.80 | | |
| [B] Receiving Cancer Treatment | 7 (44) | 2 (6) | **15.75 (1.75-141.39)** | **0.01** | **11.24 (1.72-73.28)** | **0.01** |
| *Charlson Comorbidity Index (CCI)* | | | | | | |
| 0-3 | 4 (25) | 9 (26) | Reference | | | |
| ≥ 4 | 12 (75) | 25 (74) | 1.08 (0.28-4.23) | 0.91 | | |
| History of MRSA Colonization | 6 (38) | 16 (47) | 0.68 (0.20-2.28) | 0.53 | | |
| *Presumed Source of MRSA BSI* | | | | | | |
| [C] Skin Source | 4 (25) | 7 (21) | 1.29 (0.32-5.24) | 0.73 | | |
| Pneumonia | 1 (6) | 6 (18) | 0.31 (0.03-2.83) | 0.30 | | |
| [*, †] Vascular access | 9 (56) | 9 (26) | **3.57 (1.03-12.43)** | **0.05** | | |
| Other/Undetermined | 2 (13) | 12 (35) | 0.26 (0.05-1.35) | 0.11 | | |
| Persistent Bacteremia (≥ 5 Days) | 2 (13) | 9 (26) | 0.40 (0.08-2.10) | 0.28 | | |
| ICU Admission Prior to BSI | 4 (25) | 3 (9) | 3.44 (0.67-17.73) | 0.14 | | |
| Intubated Prior to MRSA BSI | 4 (25) | 2 (6) | 5.33 (0.86-33.00) | 0.07 | | |

375 **Bold** = significant at ≤ 0.05
376 Abbreviations: BSI, bloodstream infection; HIV, human immunodeficiency virus; ICU, intensive care unit; IV, intravenous; NHSN, National Healthcare Safety
377 Network.
378 [A] Includes devices such as pacemaker, any vascular access, orthopedic hardware, foley catheter, arteriovenous graft placement, percutaneous endoscopic
379 gastronomy (PEG), ostomy, or any type of urinary collection at the time of first positive bloodstream infection.
380 [B] Includes patients actively receiving cancer treatment through a central venous catheter prior to bacteremia in the outpatient or inpatient setting.
381 [C] Skin source includes skin and soft tissue infections, thrombophlebitis due to peripheral IV catheters
382 * Variable not included in the multivariate analysis in order to prevent collinearity between receiving cancer treatment and vascular access.
383 † Vascular access devices include: non-tunneled central venous catheter, tunneled catheter (hickman or permacath), implanted port, peripherally inserted central
384 catheter (PICC line), as well as arteriovenous graft (AVG) and fistula (AVF).

# References

Anderson R, Rosenberg A, Garg S, Nahass J, Nenos A, Egorova N, Rowland J, Mari J, LoPachin V. 2019. Establishing the Foundation to Support Health System Quality Improvement: Using a Hand Hygiene Initiative to Define the Process. *J Patient Saf*. http://dx.doi.org/10.1097/PTS.0000000000000578.

Center for Disease Control and Prevention. 2018. Multidrug-Resistant Organism & Clostridioides difficile Infection (MDRO/CDI) Module.

Dupper AC, Sullivan MJ, Chacko KI, Mishkin A, Ciferri B, Kumaresh A, Caban AB, Oussenko I, Beckford C, Zeitouni NE, et al. 2019. Blurred Molecular Epidemiological Lines Between the Two Dominant Methicillin-Resistant Staphylococcus aureus Clones. *Open Forum Infectious Diseases* **6**. https://www.ncbi.nlm.nih.gov/pmc/articles/PMC6735859/ (Accessed September 25, 2019).

Eyre DW, Golubchik T, Gordon NC, Bowden R, Piazza P, Batty EM, Ip CLC, Wilson DJ, Didelot X, O'Connor L, et al. 2012. A pilot study of rapid benchtop sequencing of Staphylococcus aureus and Clostridium difficile for outbreak detection and surveillance. *BMJ Open* **2**. http://dx.doi.org/10.1136/bmjopen-2012-001124.

Hadfield J, Megill C, Bell SM, Huddleston J, Potter B, Callender C, Sagulenko P, Bedford T, Neher RA. 2018. Nextstrain: real-time tracking of pathogen evolution. *Bioinformatics* **34**: 4121–4123.

Harris SR, Feil EJ, Holden MTG, Quail MA, Nickerson EK, Chantratita N, Gardete S, Tavares A, Day N, Lindsay JA, et al. 2010. Evolution of MRSA during hospital transmission and intercontinental spread. *Science* **327**: 469–474.

Köser CU, Holden MTG, Ellington MJ, Cartwright EJP, Brown NM, Ogilvy-Stuart AL, Hsu LY, Chewapreecha C, Croucher NJ, Harris SR, et al. 2012. Rapid whole-genome sequencing for investigation of a neonatal MRSA outbreak. *N Engl J Med* **366**: 2267–2275.

Lees JA, Harris SR, Tonkin-Hill G, Gladstone RA, Lo SW, Weiser JN, Corander J, Bentley SD, Croucher NJ. 2019. Fast and flexible bacterial genomic epidemiology with PopPUNK. *Genome Res* **29**: 304–316.

Merrer J, Santoli F, Vecchi CA-D, Tran B, De Jonghe B, Outin H. 2000. "Colonization Pressure" and Risk of Acquisition of Methicillin-Resistant Staphylococcus aureus in a Medical Intensive Care Unit. *Infect Control Hosp Epidemiol* **21**: 718–723.

Ondov BD, Treangen TJ, Melsted P, Mallonee AB, Bergman NH, Koren S, Phillippy AM. 2016. Mash: fast genome and metagenome distance estimation using MinHash. *Genome Biol* **17**: 132.

Otter JA, Yezli S, French GL. 2011. The role played by contaminated surfaces in the transmission of nosocomial pathogens. *Infect Control Hosp Epidemiol* **32**: 687–699.

421 Otter JA, Yezli S, Salkeld JAG, French GL. 2013. Evidence that contaminated surfaces
422 contribute to the transmission of hospital pathogens and an overview of strategies to
423 address contaminated surfaces in hospital settings. *Am J Infect Control* **41**: S6–11.

424 SAS Institute. 2013. *Base SAS 9.4 Procedures Guide: Statistical Procedures, Second Edition*.

425 Senn L, Clerc O, Zanetti G, Basset P, Prod'hom G, Gordon NC, Sheppard AE, Crook DW,
426 James R, Thorpe HA, et al. 2016. The Stealthy Superbug: the Role of Asymptomatic
427 Enteric Carriage in Maintaining a Long-Term Hospital Outbreak of ST228
428 Methicillin-Resistant Staphylococcus aureus. *MBio* **7**: e02039–15.

429 Sullivan MJ, Altman DR, Chacko KI, Ciferri B, Webster E, Pak TR, Deikus G, Lewis-Sandari M,
430 Khan Z, Beckford C, et al. 2019. A Complete Genome Screening Program of Clinical
431 Methicillin-Resistant Staphylococcus aureus Isolates Identifies the Origin and Progression
432 of a Neonatal Intensive Care Unit Outbreak. *J Clin Microbiol* **57**.
433 http://dx.doi.org/10.1128/JCM.01261-19.

434 Treangen TJ, Ondov BD, Koren S, Phillippy AM. 2014. The Harvest suite for rapid core-genome
435 alignment and visualization of thousands of intraspecific microbial genomes. *Genome Biol*
436 **15**: 524.

437 Young BC, Golubchik T, Batty EM, Fung R, Larner-Svensson H, Votintseva AA, Miller RR,
438 Godwin H, Knox K, Everitt RG, et al. 2012. Evolutionary dynamics of Staphylococcus
439 aureus during progression from carriage to disease. *Proc Natl Acad Sci U S A* **109**:
440 4550–4555.

441 Zakhour R, Chaftari A-M, Raad II. 2016. Catheter-related infections in patients with
442 haematological malignancies: novel preventive and therapeutic strategies. *Lancet Infect Dis*
443 **16**: e241–e250.

444 Zhou Z, Alikhan N-F, Sergeant MJ, Luhmann N, Vaz C, Francisco AP, Carriço JA, Achtman M.
445 2018. GrapeTree: visualization of core genomic relationships among 100,000 bacterial
446 pathogens. *Genome Res* **28**: 1395–1404.

# Supplemental Figures

**A**

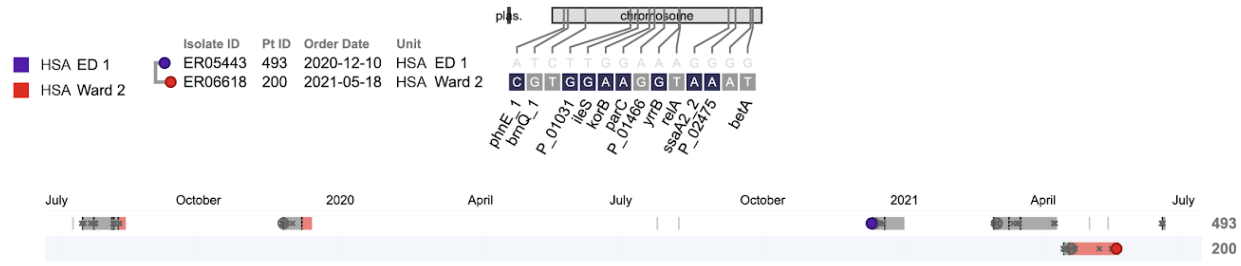


**B**

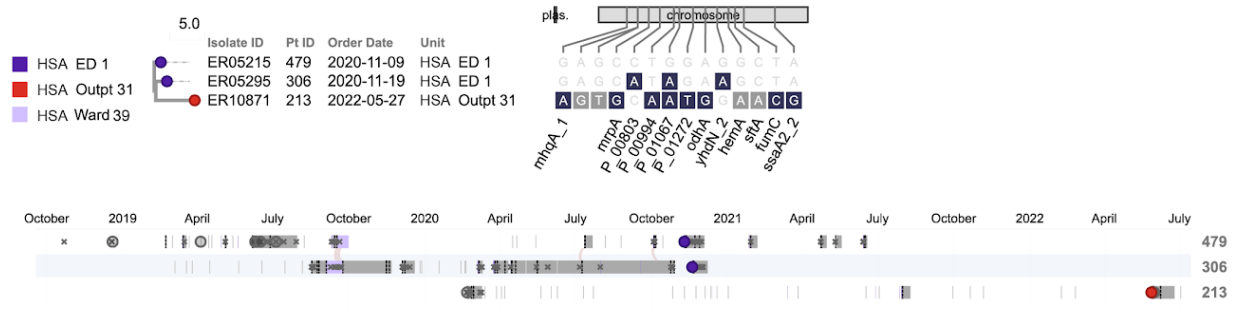


**C**

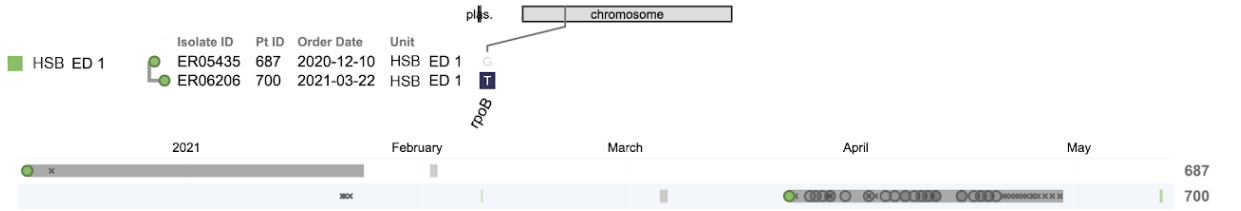


**D**

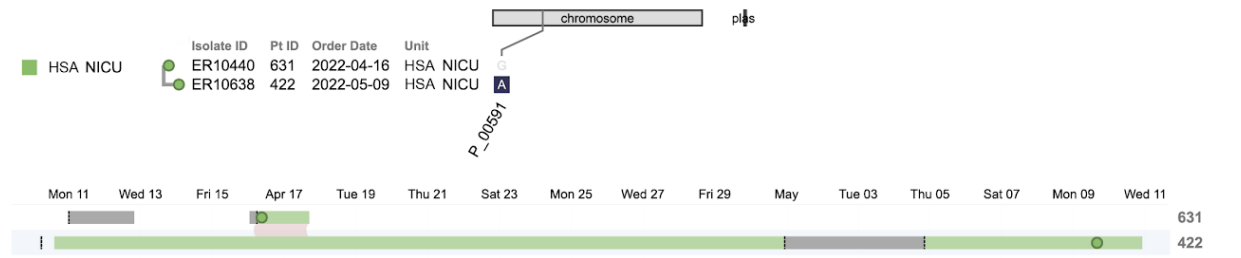

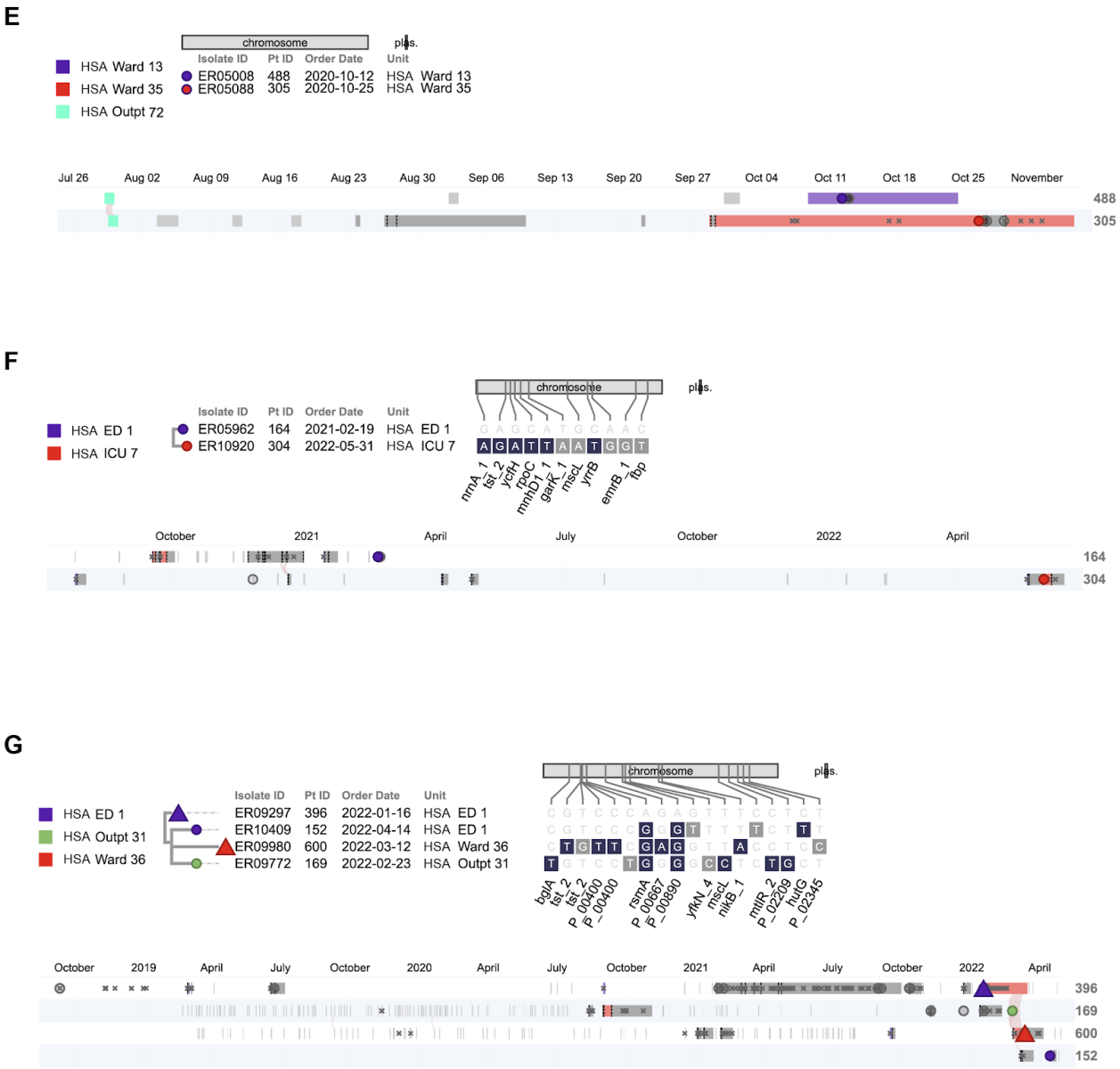


448 Figure S1. Other clonal clusters identified by PathoSPOT analysis

449 Phylogenetic trees of core genomes and epidemiologic timelines created by the
450 “dendro-timeline” visualization in PathSPOT for the seven smaller clonal clusters identified in
451 our study **(A-G)**. Layout and drawing conventions are as in Figures 3A and B. All date
452 information in this figure was recoded to protect health information..

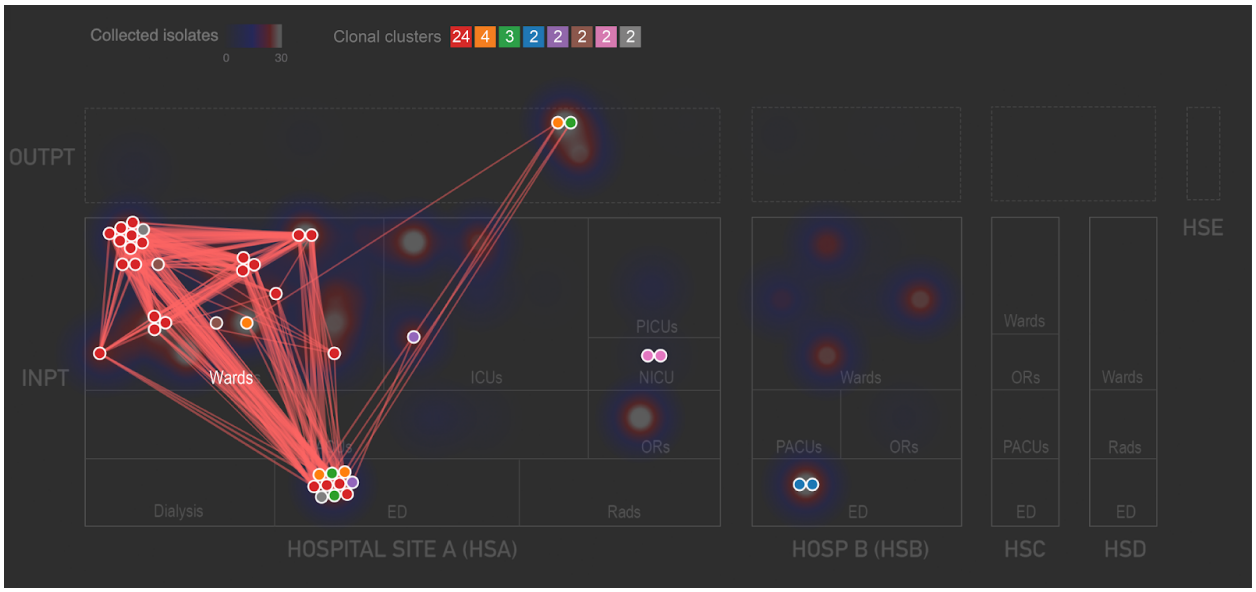


453 Figure S2. Network layout view of clonal clusters

454 The PathoSPOT network layout shows spatial relationships among patients in each of the 8
455 clusters, using the threshold of ≤15 SNVs across the entire 24 months of the dataset, and only
456 the first related isolate from each patient. Nodes are colored by clonal cluster, as indicated in the
457 legend at top center, which also lists the numbers of nodes in each cluster. Nodes are laid out
458 spatially by hospital and ward where the patient was sampled, with ward types grouped together
459 (labeled boxes), and nodes from the same ward placed adjacent to one another (the position of
460 each anonymized ward within the box is arbitrary). Genomic links underneath the threshold are
461 depicted as red lines, with many clusters spread across different wards and ward types.
462 Underneath the network map, the total number of positive cultures collected from each location
463 is depicted as a shaded density plot, with the color scale depicted at top left; this highlights
464 heavily sampled locations.